Essential Regulation of CNS Angiogenesis by the Orphan G Protein–Coupled Receptor GPR124

Frank Kuhnert *et al.*

Science **330**, 985 (2010);
DOI: 10.1126/science.1196554

Science (print ISSN 0036-8075; online ISSN 1095-9203) is published weekly, except the last week in December, by the American Association for the Advancement of Science, 1200 New York Avenue NW, Washington, DC 20005.

tality or severe complications after pertussis infection. In the extreme (and logistically unfeasable) situation where 75% of the 11 and older population are immunized at 5-yearly intervals, incidence reduction approaches only 15%. These results raise important questions about the epidemiological effectiveness and financial prudence of booster programs for adolescents and adults.

Our model ignores the myriad complexities that have been proposed as explanations for recent pertussis epidemiology. Critically, it ignores loss of immunity. This assumption is reasonable and has its basis in empirical evidence. Equivalent parameterization of an SIRS model that assumes temporary immunity reveals q—the probability of infection given contact—to be age dependent and to decay exponentially beyond ages 4 to 5 (fig. S5). Hence, the age-specific Sweden data provide strong support for the stated minimal transmission impact of repeat asymptomatic infections (*28*), which has been inferred from aggregate epidemiological data in other countries (*8*, *29*, *30*). It remains to be seen whether the explanatory power of our simple yet predictive model will substantially increase with the inclusion of additional complexities, be they age-dependent effects (e.g., differential transmissibility, susceptibility, and observability) or refinements of the contact network (e.g., household and spatial structuring).

Since the pioneering work of Fine and Clarkson, the impact of pertussis vaccines has been the subject of much debate (*31*). The focus of contention has been whether vaccination protects against transmission or merely disease. Our analysis strongly points to the former: The pronounced drop in incidence in the infant, toddler, and adult groups after infant immunization is indicative of reduced pertussis circulation and increased herd immunity (*13*). Our findings also point toward a minimal transmission role for adults, due to the strong assortativity of contacts among the young (Fig. 2D). Hence, we conclude that adults are not the missing piece of the puzzle they have been made out to be (*23*). Our results suggest that contact structure is the pivotal element for understanding the epidemiology of pertussis and, it is likely, other directly transmitted infectious diseases.

References and Notes

1. L. P. Celentano, M. Massari, D. Paramatti, S. Salmaso, A. E. Tozzi; EUVAC-NET Group, *Pediatr. Infect. Dis. J.* **24**, 761 (2005).
2. N. S. Crowcroft, C. Stein, P. Duclos, M. Birmingham, *Lancet Infect. Dis.* **3**, 413 (2003).
3. N. S. Crowcroft, R. G. Pebody, *Lancet* **367**, 1926 (2006).
4. J. D. Cherry, *Pediatrics* **112**, 405 (2003).
5. H. O. Hallander, A. Advani, D. Donnelly, L. Gustafsson, R.-M. Carlsson, *J. Clin. Microbiol.* **43**, 2856 (2005).
6. F. R. Mooi, I. H. van Loo, A. J. King, *Emerg. Infect. Dis.* **7** (suppl.), 526 (2001).
7. T. Tan, E. Trindade, D. Skowronski, *Pediatr. Infect. Dis. J.* **24** (suppl.), S10 (2005).
8. H. J. Wearing, P. Rohani, *PLoS Pathog.* **5**, e1000647 (2009).
9. S. B. Omer *et al.*, *JAMA* **296**, 1757 (2006).
10. B. Ntezayabo, G. De Serres, B. Duval, *Pediatr. Infect. Dis. J.* **22**, 22 (2003).
11. V. Romanus, R. Jonsell, S. O. Bergquist, *Pediatr. Infect. Dis. J.* **6**, 364 (1987).
12. E. J. Gangarosa *et al.*, *Lancet* **351**, 356 (1998).
13. R.-M. Carlsson, B. Trollfors, *Vaccine* **27**, 5709 (2009).
14. J. Mossong *et al.*, *PLoS Med.* **5**, e74 (2008).
15. D. M. Skowronski *et al.*, *J. Infect. Dis.* **185**, 1448 (2002).
16. D. Güris *et al.*, *Clin. Infect. Dis.* **28**, 1230 (1999).
17. D. Schenzle, *IMA J. Math. Appl. Med. Biol.* **1**, 169 (1984).
18. R. Anderson, R. May, *Infectious Diseases of Humans: Dynamics and Control* (Oxford Univ. Press, Oxford, 1991).
19. M. Keeling, P. Rohani, *Modelling Infectious Diseases* (Princeton Univ. Press, Princeton, NJ, 2008).
20. R. M. Anderson, R. M. May, *J. Hyg. (London)* **94**, 365 (1985).
21. W. J. Edmunds, N. J. Gay, M. Kretzschmar, R. G. Pebody, H. Wachmann; ESEN Project. European Sero-epidemiology Network, *Epidemiol. Infect.* **125**, 635 (2000).
22. J. Wallinga, J. C. M. Heijne, M. Kretzschmar, *PLoS Med.* **2**, e316 (2005).
23. J. D. Cherry, L. J. Baraff, E. Hewlett, *West. J. Med.* **150**, 319 (1989).
24. K. Kretsinger *et al.*, *MMWR Recomm. Rep.* **55** (RR-17), 1 (2006).
25. J. D. Nelson, *Am. J. Dis. Child.* **132**, 371 (1978).
26. J. G. Deville *et al.*, *Clin. Infect. Dis.* **21**, 639 (1995).
27. C. H. von König, S. Halperin, M. Riffelmann, N. Guiso, *Lancet Infect. Dis.* **2**, 744 (2002).
28. J. Schellekens, C. H. von König, P. Gardner, *Pediatr. Infect. Dis. J.* **24** (suppl.), S19 (2005).
29. H. Broutin, P. Rohani, J.-F. Guégan, B. T. Grenfell, F. Simondon, *Vaccine* **22**, 594 (2004).
30. H. Broutin, C. Viboud, B. T. Grenfell, M. A. Miller, P. Rohani, *Proc. Biol. Sci.* **277**, 3239 (2010).
31. P. E. Fine, J. A. Clarkson, *Lancet* **1**, 666 (1982).
32. T. Eidlitz-Markus, M. Mimouni, A. Zeharia, *Clin. Pediatr. (Phila.)* **46**, 718 (2007).

33. We thank three anonymous reviewers for comments. P.R. and A.A.K. are supported by the Research and Policy in Infectious Disease Dynamics program of the Science and Technology Directorate, Department of Homeland Security, and the Fogarty International Center, National Institutes of Health. P.R. was also supported by the Vaccine Modeling Initiative of the Bill & Melinda Gates Foundation.

Supporting Online Material

www.sciencemag.org/cgi/content/full/330/6006/982/DC1
Methods
Figs. S1 to S14
References

23 June 2010; accepted 11 October 2010
10.1126/science.1194134

Essential Regulation of CNS Angiogenesis by the Orphan G Protein–Coupled Receptor GPR124

Frank Kuhnert,[1]* Michael R. Mancuso,[1] Amir Shamloo,[2] Hsiao-Ting Wang,[1] Vir Choksi,[3] Mareike Florek,[4] Hua Su,[5] Marcus Fruttiger,[6] William L. Young,[7] Sarah C. Heilshorn,[8] Calvin J. Kuo[1]†

The orphan G protein–coupled receptor (GPCR) GPR124/tumor endothelial marker 5 is highly expressed in central nervous system (CNS) endothelium. Here, we show that complete null or endothelial-specific GPR124 deletion resulted in embryonic lethality from CNS-specific angiogenesis arrest in forebrain and neural tube. Conversely, GPR124 overexpression throughout all adult vascular beds produced CNS-specific hyperproliferative vascular malformations. In vivo, GPR124 functioned cell-autonomously in endothelium to regulate sprouting, migration, and developmental expression of the blood-brain barrier marker Glut1, whereas in vitro, GPR124 mediated Cdc42-dependent directional migration to forebrain-derived, vascular endothelial growth factor–independent cues. Our results demonstrate CNS-specific angiogenesis regulation by an endothelial receptor and illuminate functions of the poorly understood adhesion GPCR subfamily. Further, the functional tropism of GPR124 marks this receptor as a therapeutic target for CNS-related vascular pathologies.

Organ-specific vascular beds form through angiogenesis, followed by substantial anatomic and molecular differentiation to support various physiologic requirements (*1*, *2*). The central nervous system (CNS) vasculature is highly specialized, with a blood-brain barrier (BBB), extensive pericyte coverage, reciprocal interactions with neurons and glia, and function as a neural stem cell niche (*3*–*5*). In the developing CNS, the perineural vascular plexus (PNVP) surrounds the ventral neural tube at embryonic day 7.5 (E7.5) to E8.5. By E11.5, angiogenic endothelial sprouts invade the neuroepithelium from the pial surface to periventricular areas and branch, generating the periventricular vascular plexus

[1]Department of Medicine, Hematology Division, Stanford University, Stanford, CA 94305, USA. [2]Department of Mechanical Engineering, Stanford University, Stanford, CA 94305, USA. [3]Department of Bioengineering, Stanford University, Stanford, CA 94305, USA. [4]Division of Blood and Marrow Transplantation, Stanford University, Stanford, CA 94305, USA. [5]Center for Cerebrovascular Research, Department of Anesthesia and Perioperative Care, University of California San Francisco (UCSF), San Francisco, CA 94110, USA. [6]UCL Institute of Ophthalmology, University College London, London EC1V 9EL, UK. [7]Center for Cerebrovascular Research, Department of Anesthesia and Perioperative Care, Department of Neurological Surgery, Department of Neurology, University of California, San Francisco, San Francisco, CA 94110 USA. [8]Department of Materials Science and Engineering, Stanford University, Stanford, CA 94305, USA.

*Present address: Regeneron Pharmaceuticals, Tarrytown, NY 10591, USA.
†To whom correspondence should be addressed. E-mail: cjkuo@stanford.edu

(PVVP) (*6*, *7*). This angiogenic invasion has been proposed to occur concomitantly with barriergenesis, the acquisition of BBB properties (*8*, *9*). Heretofore, endothelial receptors mediating CNS-specific angiogenesis have not been described.

We investigated GPR124 or tumor endothelial marker 5 (TEM5), which is an orphan G protein–coupled receptor (GPCR) with a large ectodomain belonging to the adhesion GPCR subfamily (fig. S1A) (*10*). GPR124 (TEM5) was initially identified as differentially expressed in tumor vasculature (*11*, *12*) and in genomic analysis of GPCR loci (*13*). During mouse embryogenesis, GPR124 was expressed in both endothelial cells and pericytes, most prominently in brain and neural tube (fig. S1, B to L), and to lesser degrees in non-CNS embryonic organs, including the liver, heart, and kidney (fig S2). GPR124 was also expressed in embryonic epithelium of lung and esophagus and in mesenchyme (fig. S2). In contrast, adult GPR124 expression was exclusively vascular in tissues examined, with endothelial expression in CNS including the brain and retina (fig. S3) and more widespread pericyte expression in the brain and organs, including the kidney, pancreas, and corpus luteum (fig. S4).

To examine the function of this orphan receptor, we generated a GPR124 lacZ knock-in null allele, which displayed a vascular embryonic expression pattern upon β-galactosidase staining of heterozygous embryos at E10.5 (figs. S5 and S6). No viable adult GPR124$^{-/-}$ (GPR124$^{lacZ/lacZ}$) mice were obtained (fig. S7). Beginning at E11, GPR124$^{-/-}$ embryos exhibited completely penetrant, progressive CNS hemorrhage originating in forebrain telencephalon and ventral neural tube (Fig. 1, A to D, and figs. S7 and S8), with resultant embryonic lethality from E15.5 onward (fig. S7). Paralleling sites of hemorrhage, GPR124$^{-/-}$ embryos at E11.5 displayed selective CNS-specific vascular patterning defects, with markedly reduced angiogenic sprouting into the forebrain telencephalon and thickening of the underlying PNVP, rendering the telencephalon virtually avascular (Fig. 1, E to H). By E14.5, this culminated in formation of basally localized glomeruloid malformations and resultant distally unvascularized telencephalon in GPR124$^{-/-}$ embryos. In contrast, wild-type mice showed efficient migration of endothelial cells to the subventricular zone (SVZ) (Fig. 1, M to R). Similar striking angiogenic deficits with characteristic hemorrhagic glomeruloid malformations were also seen in GPR124$^{-/-}$ ventral neural tube and forebrain ganglionic eminences (Fig. 1, I to L). GPR124 deletion did not impair angiogenic sprouting into the embryonic diencephalon, mid- and hindbrain, or the vascularization of nonneural tissues (Fig. 1, E to F and M to N, and figs. S9 and S10). Electron microscopy (EM) of GPR124$^{-/-}$ CNS vascular malformations revealed numerous packed endothelial cells with scant cytoplasm, enveloped

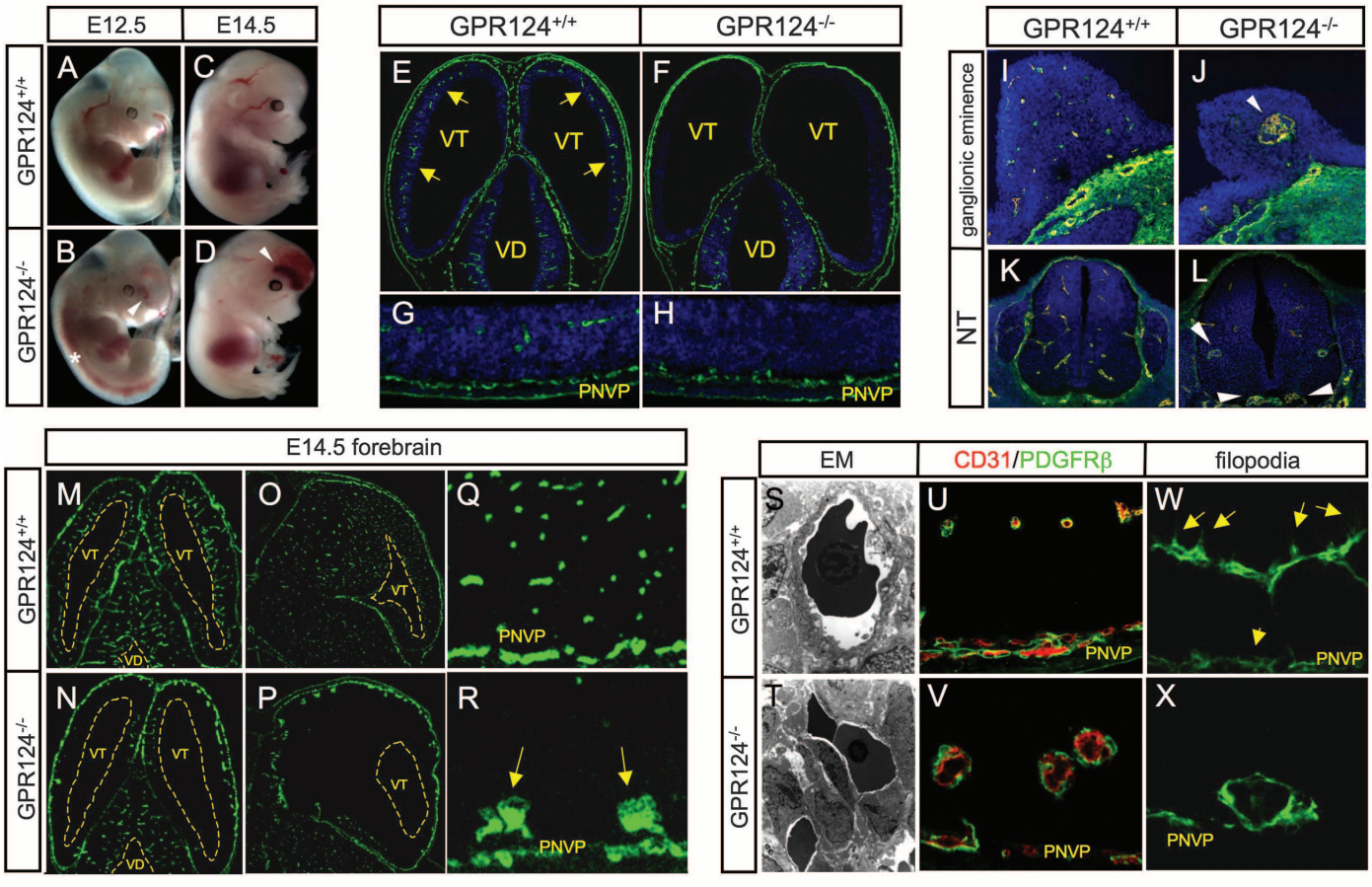

Fig. 1. CNS vascular patterning defects in GPR124$^{-/-}$ embryos. (**A** to **D**) GPR124$^{-/-}$ embryos manifested progressive hemorrhage confined to forebrain telencephalon (arrowheads) and neural tube (asterisk). (**E** and **G**) Wild-type E11.5 embryos exhibited efficient sprouting angiogenesis (arrows) from the PNVP into the telencephalon, which was (**F** to **H**) completely ablated in GPR124$^{-/-}$ embryos that exhibited PNVP thickening only. Green indicates CD31 immunofluorescence (IF). (**I** to **L**) Large, glomeruloid vascular malformations (arrowheads) and absence of a vascular network were observed in E11.5 GPR124$^{-/-}$ forebrain ganglionic eminences and ventral neural tube (CD31 IF). (**M** to **R**) By E14.5, GPR124$^{-/-}$ telencephalon was essentially devoid of a mature capillary network, with glomeruloid malformations abutting the pia/PNVP, whereas the diencephalon was unaffected [(M) to (N), transverse; (O) to (P), sagittal; vascular malformations (arrows); (Q) and (R), CD31 IF]. (**S** to **X**) Glomeruloid malformations were irregular, multilayer endothelial aggregates versus single-layer capillaries in controls [(S) and (T), EM 4300×], with normal peripheral PDGFRβ^{+} pericyte investment [(U) and (V)] but lacked ventricularly directed endothelial filopodia (arrows) [(W) and (X), CD31 IF]. VD, ventricle diencephalons; VT, ventricle telencephalon; blue, 4′,6′-diamidino-2-phenylindole.

by PDGFRβ^{+} pericytes (Fig. 1, S to V). Further, GPR124$^{-/-}$ endothelium showed markedly reduced-to-absent filopodial extensions that when present extended laterally rather than toward the ventricles as in wild type (Fig. 1, W to X). Proliferation, apoptosis, and vascular endothelial growth factor (VEGF) receptor expression were grossly unaltered in GPR124$^{-/-}$ vascular malformations (fig. S11). We conclude that GPR124 displays a pronounced functional tropism for the CNS and is essential for developmental angiogenic sprouting into forebrain and neural tube.

Mice in which Wnt7/β-catenin had been knocked out (Wnt7/β-catenin knockout mice) with CNS angiogenesis deficits exhibit defective developmental expression of the BBB-specific glucose transporter Glut1, suggesting that acquisition of BBB markers may be coupled to developmental brain angiogenesis (*8*, *9*). Glut1 expression was similarly absent in GPR124$^{-/-}$ endothelium in forebrain upon immunofluorescence and quantitative polymerase chain reaction (PCR) analysis of purified primary forebrain GPR124$^{-/-}$ endothelial cells (ECs) (Fig. 2, A to E); expression in mid- and hindbrain was unaffected. Compensatory neuroepithelial Glut-1 up-regulation was present (Fig. 2,

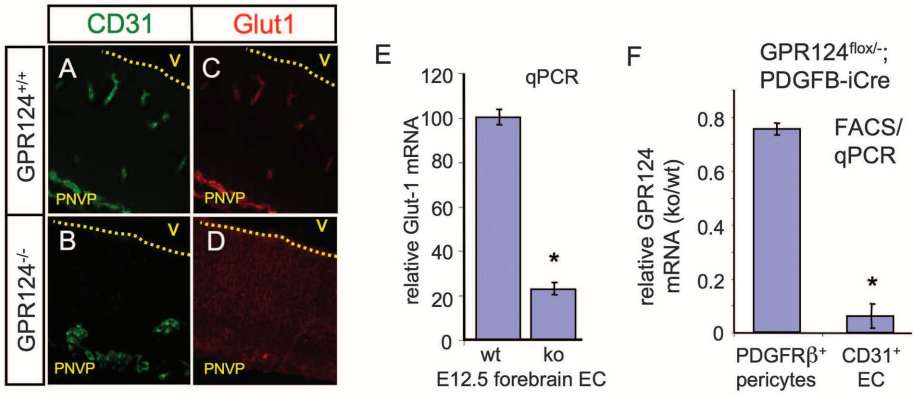

Fig. 2. GPR124 functions cell-autonomously in endothelium. (**A** to **D**) Expression of Glut1 is lost in GPR124$^{-/-}$ CNS endothelium, with compensatory Glut1 up-regulation in neuroepithelium (E12.5). Glut1 is strongly down-regulated in FACS-isolated, GPR124$^{-/-}$ telencephalic endothelium. (**E**) Quantitative PCR, $n = 9$ determinations, E12.5. Selective deletion of GPR124 in FACS-isolated forebrain CD31^{+} endothelium but not PDGFRβ+ pericytes. (**F**) Quantitative PCR, $n = 6$ determinations, E 12.5. (**G** to **L**) E12.5 GPR124$^{flox/-}$;PDGFB-iCre embryos exhibit forebrain hemorrhaging, formation of PNVP-associated glomeruloid vascular malformations, and endothelial Glut1 down-regulation, recapitulating the global GPR124 deletion phenotype. Error bars are ± 1 SD.

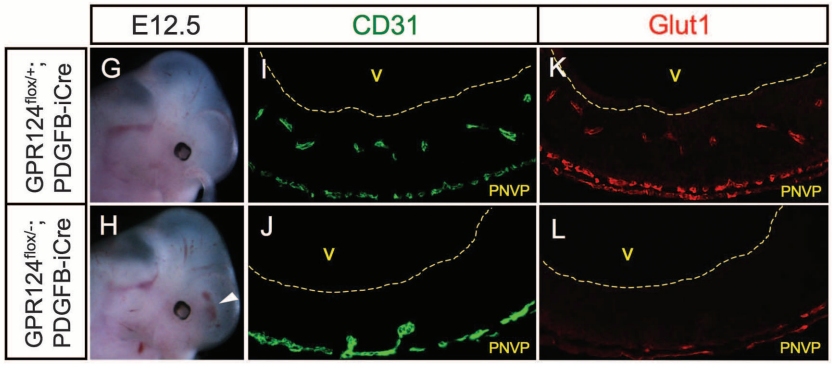

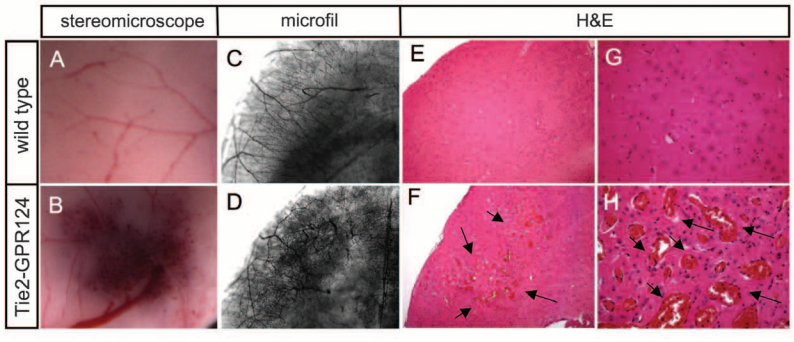

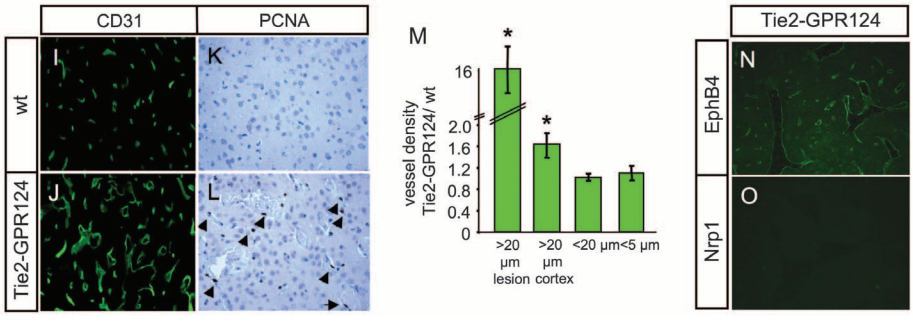

Fig. 3. CNS vascular malformations in adult (12 months old) Tie2-GPR124 transgenic animals. (**A** to **D**) Focally increased red blood cell accumulation in Tie2-GPR124 cerebral cortex [(A) and (B)] corresponded to increased vascular density and tortuous, enlarged vessels upon microfil vascular casting [(C) and (D)]. (**E** to **H**) Hematoxylin and eosin staining of a hypervascular area (arrows) in Tie2-GPR124 cortex [(E) and (F) 100×] revealed dramatically enlarged, engorged thin-walled vessels with intervening neural tissue reminiscent of venous angiomas [(G) and (H) 400×]. (**I** to **M**) Tie2-GPR124 transgenics exhibited increased CD31^{+} microvessel density and markedly enlarged [(I), (J), and (M)] and hyperproliferative vascular malformations versus wild-type controls [(K) and (L); arrowheads denote PCNA^{+} cells]. Tie2-GPR124 CNS vascular malformations expressed the venous marker EphB4 but not the arterial receptor Nrp1 (**N** and **O**). Error bars are ± 1 SD.

C and D), as also seen in Wnt7/β-catenin knockout mice (*8*, *9*).

To demonstrate endothelial cell-autonomous function of GPR124 in regulating CNS angiogenesis, we generated a floxed exon 1 GPR124 allele ($GPR124^{flox}$) and crossed to PDGFB-iCre mice so as to allow endothelial CreER-mediated deletion (*14*). Accordingly, E12.5 $GPR124^{flox/-}$;PDGFB-iCre embryos demonstrated selective GPR124 deletion in endothelium but not pericytes through fluorescence-activated cell sorting (FACS) and quantitative PCR (Fig. 2F). $GPR124^{flox/-}$;PDGFB-iCre mice fully recapitulated the GPR124 null phenotype with forebrain hemorrhage, CNS angiogenic arrest, basally localized glomeruloid malformations, and loss of endothelial Glut1 expression (Fig. 2, G to L). Identical results were obtained with an independent vascular deletion strategy in $GPR124^{flox/-}$;Tie2-Cre mice (fig. S12). These results indicate that GPR124 functions cell-autonomously in CNS endothelium, with Glut1 as a developmentally regulated downstream locus.

To analyze gain-of-function phenotypic outcomes, we generated transgenic mice overexpressing GPR124 cDNA from the Tie2 promoter/long-enhancer active in embryonic and adult endothelium (*15*). Tie2-GPR124 transgenic mice were viable and fertile. The mutant mice exhibited enhanced brain vascular GPR124 immunofluorescence versus nontransgenic littermates and displayed ectopic GPR124 expression throughout the microvasculature of adult organs that do not normally express GPR124, such as the heart and liver (fig. S13). Despite widespread GPR124 overexpression, Tie2-GPR124 animals displayed a progressive brain-specific vascular phenotype characterized by enlarging oligo-focal areas of hypervascularity that were predominantly cortical (>90%, with ~10% in the cerebellum) and presented with ~70% penetrance by 12 months of age, paralleling the forebrain telencephalon distribution of $GPR124^{-/-}$ malformations (Fig. 3, A to H and M); non-CNS organs were unaffected (fig. S14). These lesions consisted of tangled, thin-walled, CD31-positive, grossly dilated hyperproliferative capillaries with associated $PDGFR\beta^{+}$ pericytes (Fig. 3, I to L, and fig. S15). The vascular malformations exhibited intervening neural tissue reminiscent of venous angiomas and expressed the venous marker EphB4 but not the arterial marker Nrp1 (Fig. 3, N and O). Calcifications were frequently associated (fig. S15E), and transgenic mice occasionally exhibited neurologic symptoms, such as ataxia. Thus, both the Tie2-GPR124–overexpressing mice and

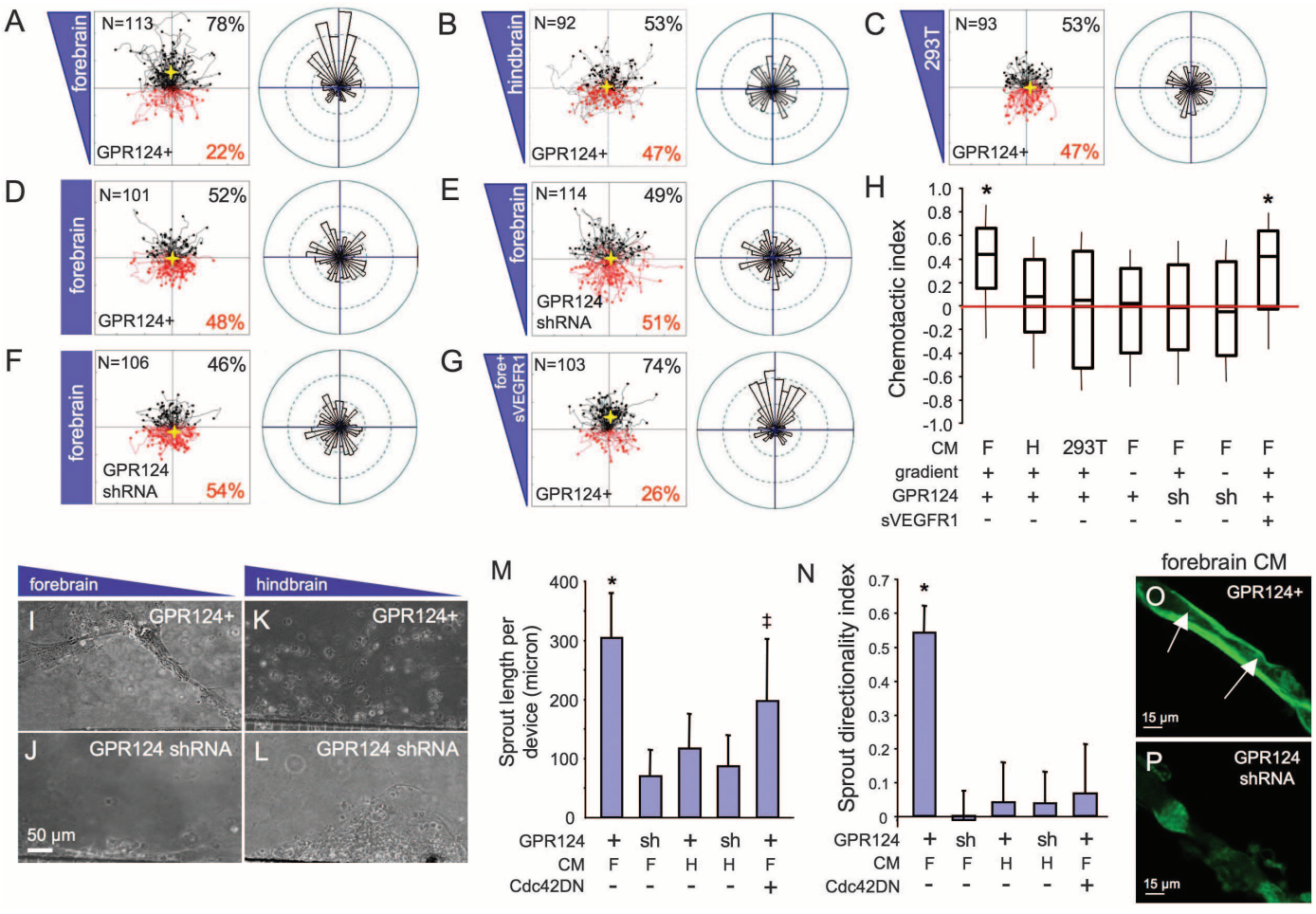

Fig. 4. GPR124 regulates CNS endothelial migration and sprout formation in vitro. Motility of the GPR124-expressing brain endothelial line bEND3 was monitored with real-time video microscopy in a microfluidic migration chamber, allowing extremely stable, shear-minimized linear chemoattractant gradients. (**A** to **C**) GPR124-overexpressing bEND3 cells ($GPR124^{+}$) exhibited directed migration toward gradients of conditioned medium (CM) from cultured E12.5 forebrain cortical cells but migrated randomly to equivalent hindbrain or HEK293T CM [tracks of individual cells (left) and angular histograms (right) are shown]. (**D** to **F**) No directed migration was observed with even distribution of forebrain CM across the microfluidic chamber (no gradient), or GPR124 shRNA; (**G**) migration was further insensitive to a recombinant soluble VEGFR1 ectodomain (400 ng/ml), indicating VEGF-independence. (**H**) Box plot of chemotactic indices of bEND3 migration (center line, median; boxes, upper and lower quartiles, $*P < 0.001$). (**I** to **L**) In a sprout formation assay, $GPR124^{+}$ bEND3 displayed collective cell migration and robust formation of stable sprouts toward forebrain CM gradients, but not to hindbrain CM nor upon GPR124 shRNA knockdown. (**M** and **N**) Dominant-negative Cdc42N17 inhibited sprout directionality but not elongation ($*P < 0.05$; ‡ indicates not significant). $GPR124^{+}$ sprouts toward forebrain CM–contained stable, contiguous lumens, whereas rare GPR124 shRNA sprouts were unstable and failed to lumenize. (**O** and **P**) Confocal microscopy. F, forebrain CM; H, hindbrain CM. Error bars are ± 1 SE. $*P < 0.05$; $n = 3$ to 5 chambers per condition.

GPR124$^{-/-}$ embryos displayed angiogenic phenotypes highly restricted to the CNS vasculature.

The angiogenic defects in GPR124$^{-/-}$ forebrain but not mid- or hindbrain suggested that GPR124 could mediate endothelial migration toward forebrain-enriched regional guidance cues within the embryonic CNS. The GPR124-expressing brain endothelial cell line bEND3 was used in a microfluidic migration chamber, allowing extremely stable, shear-minimized linear chemoattractant gradients and real-time video microscopy of cellular motility (fig. S16A) (*16*). GPR124-overexpressing bEND3 cells (GPR124^{+}) (fig. S16B) exhibited directed migration in microfluidic chambers toward gradients of conditioned medium from cultured E12.5 forebrain cortical cells (F) but migrated randomly when presented with equivalent hindbrain preparations (H) or with human embryonic kidney (HEK) 293T–conditioned medium (chemotactic indices of 0.44, 0.08, and 0.02, respectively) (Fig. 4, A to C and H, and fig. S17). Further, directed migration was not observed when forebrain-conditioned medium was evenly distributed across the microfluidic chamber (no gradient), or upon GPR124^{-} short hairpin RNA (shRNA) knockdown (Fig. 4, D to F and H, and fig. S17). GPR124^{+} bEND3 migration to the forebrain CM gradient was insensitive to a recombinant soluble VEGFR1 ectodomain, which is consistent with VEGF-independence. (Fig. 4, G and H, and fig. S17).

We also used a second microfluidic assay in which bEND3 cells sprouted through microcapillaries into an acellular chamber that contained a transverse gradient of chemoattractant (fig. S18). This revealed multicellular endothelial sprout elongation and directional migration toward forebrain- but not hindbrain-conditioned medium gradients that was ablated with GPR124 shRNA (Fig. 4, I to N). Cdc42 was required for GPR124-dependent directional migration but not sprout elongation, as revealed by a dominant-negative Cdc42 allele (Cdc42N17) (Fig. 4, M to N). GPR124^{+} sprouts to forebrain-conditioned medium demonstrated contiguous lumen formation upon three-dimensional confocal reconstruction, which was not observed with GPR124 shRNA (Fig. 4, O and P), paralleling lumen enlargement in Tie2-GPR124 transgenics (Fig. 3, H and J). Thus, GPR124 mediates cell-autonomous and VEGF-independent regulation of endothelial migration in response to factor (or factors) secreted from embryonic forebrain neuroepithelium.

Our studies demonstrate that GPR124 (TEM5) is a previously unknown proangiogenic, endothelial receptor with pronounced functional tropism for the CNS vasculature in both loss-of-function and gain-of-function settings. Although GPR124 was initially described as up-regulated in neoplastic (versus resting) endothelium (*11*, *12*), our work establishes its function in normal tissues as a previously unsuspected and essential regulator of CNS angiogenesis, via an endothelial cell-autonomous pathway regulating Cdc42-dependent angiogenic migration and sprouting. Despite the atretic and misoriented filopodia in GPR124 knockout vasculature, GPR124-deficient endothelium can incorporate into "tip cell" positions upon mosaic analysis (fig. S19).

Because GPR124 is expressed at all levels of the CNS vasculature, the forebrain- and ventral neural tube–specific angiogenic deficits suggest a corresponding embryonic spatial restriction of either GPR124 ligand or signaling. Further, the GPR124 phenotype indicates substantial regional heterogeneity in embryonic CNS requirements for angiogenic signals, which could operate in the context of telencephalic angiogenic gradients, as have been proposed (*17*). The spatial restriction of GPR124$^{-/-}$ angiogenesis deficits is strongly paralleled by a VEGF-independent activity mediating GPR124- and Cdc42-dependent migration to forebrain- but not hindbrain-conditioned medium. In principle, this activity could represent ligand or render competence to respond to ligand. However, this by no means excludes GPR124 interactions with nonsoluble factors such as extracellular matrix (*18*) or transmembrane proteins, or distinct mechanisms for nonangiogenic receptor functions. The progressive nature of Tie2-GPR124 vascular malformations indicates a continued sensitivity of brain endothelium to GPR124 during adulthood, with the adult temporal window possibly reflecting either moderate gain-of-function with receptor overexpression or differential sensitivity to receptor in adulthood.

Wnt/β-catenin (*8*, *9*), VEGF/Nrp1 (*19*, *20*), integrins α_v and β_8 (*21*–*23*), and Id1/Id3 (*24*) mutations impair CNS angiogenesis, often with knockout glomeruloid malformations that resemble the GPR124 phenotype (*25*). Regional regulation of angiogenesis has been reported in CXCL12/CXCR4 mutants although not in the CNS (*26*, *27*). However, as opposed to GPR124, none of these loci encode endothelial receptors with CNS functional tropism, and instead manifest vascular deficits globally or in subsets of non-CNS organs (*28*–*30*). Despite marked phenotypic overlap, GPR124 does not appear to exhibit epistasis with β-catenin (fig. S20), and we cannot exclude GPR124 function in a parallel pathway, coupling embryonic CNS angiogenesis to developmental Glut1 expression. Similar epistasis studies with Id1 and integrin β8 have also been negative (fig. S20).

The CNS enrichment of endothelial GPR124 expression, as well as the GPR124 gain- and loss-of-function angiogenesis phenotypes, suggest the potential relevance of this receptor to various CNS-related vascular pathologies, including stroke and malignancy. Certainly, the determination of potential causal relations between GPR124 and CNS vascular malformations or germinal matrix hemorrhage (*31*) in human and mouse should be worthwhile. The current analyses also provide insight into the poorly understood functions of the adhesion receptor class of GPCRs (*13*) and show how control of angiogenesis can be managed in different ways by specific organ systems, in this case with insight into angiogenesis in the CNS and development of the BBB. Similar signaling pathways may be deployed among vascular beds specific to other organ systems.

References and Notes

1. P. Carmeliet, *Nature* **438**, 932 (2005).
2. W. C. Aird, *Circ. Res.* **100**, 174 (2007).
3. P. Ballabh, A. Braun, M. Nedergaard, *Neurobiol. Dis.* **16**, 1 (2004).
4. W. M. Pardridge, *Methods Mol. Med.* **89**, 385 (2003).
5. Q. Shen *et al.*, *Science* **304**, 1338 (2004).
6. K. A. Hogan, C. A. Ambler, D. L. Chapman, V. L. Bautch, *Development* **131**, 1503 (2004).
7. R. Herken, W. Götz, K. H. Wattjes, *J. Anat.* **164**, 85 (1989).
8. J. M. Stenman *et al.*, *Science* **322**, 1247 (2008).
9. R. Daneman *et al.*, *Proc. Natl. Acad. Sci. U.S.A.* **106**, 641 (2009).
10. Materials and methods are available as supporting material on *Science* Online.
11. B. St Croix *et al.*, *Science* **289**, 1197 (2000).
12. E. B. Carson-Walter *et al.*, *Cancer Res.* **61**, 6649 (2001).
13. R. Fredriksson, D. E. Gloriam, P. J. Höglund, M. C. Lagerström, H. B. Schiöth, *Biochem. Biophys. Res. Commun.* **301**, 725 (2003).
14. S. Claxton *et al.*, *Genesis* **46**, 74 (2008).
15. T. M. Schlaeger *et al.*, *Proc. Natl. Acad. Sci. U.S.A.* **94**, 3058 (1997).
16. A. Shamloo, N. Ma, M. M. Poo, L. L. Sohn, S. C. Heilshorn, *Lab Chip* **8**, 1292 (2008).
17. A. Vasudevan, J. E. Long, J. E. Crandall, J. L. Rubenstein, P. G. Bhide, *Nat. Neurosci.* **11**, 429 (2008).
18. M. Vallon, M. Essler, *J. Biol. Chem.* **281**, 34179 (2006).
19. H. Gerhardt *et al.*, *Dev. Dyn.* **231**, 503 (2004).
20. S. Raab *et al.*, *Thromb. Haemost.* **91**, 595 (2004).
21. J. H. McCarty *et al.*, *Development* **132**, 165 (2005).
22. J. Zhu *et al.*, *Development* **129**, 2891 (2002).
23. B. L. Bader, H. Rayburn, D. Crowley, R. O. Hynes, *Cell* **95**, 507 (1998).
24. D. Lyden *et al.*, *Nature* **401**, 670 (1999).
25. M. R. Mancuso, F. Kuhnert, C. J. Kuo, *Lymphat. Res. Biol.* **6**, 173 (2008).
26. T. Ara, K. Tokoyoda, R. Okamoto, P. A. Koni, T. Nagasawa, *Blood* **105**, 3155 (2005).
27. A. F. Siekmann, C. Standley, K. E. Fogarty, S. A. Wolfe, N. D. Lawson, *Genes Dev.* **23**, 2272 (2009).
28. P. Carmeliet *et al.*, *Nature* **380**, 435 (1996).
29. N. Ferrara *et al.*, *Nature* **380**, 439 (1996).
30. A. Cattelino *et al.*, *J. Cell Biol.* **162**, 1111 (2003).
31. P. Ballabh, *Pediatr. Res.* **67**, 1 (2010).

32. We are indebted to R. Daneman, B. Barres, C. Chartier, and the Kuo laboratory for comments; J. Yuan and J. Hampton for animal husbandry and genotyping; and A. Connolly and H. Vogel for neuropathology. F.K. was supported by an American Heart Association (AHA) Postdoctoral Fellowship and M.R.M. by AHA Predoctoral Fellowship AHA09PRE2110036 and the Stanford Medical Scientist Training Program Program (National Institute of General Medical Science, NIH, GM07365). This work was also supported by NIH R21 NS070153 and AHA 10GRNT3130004 (H.S.); NIH R01NS27713 (W.L.Y.); P01NS44155 (W.L.Y. and H.S.); U.K. Medical Research Council G0501711 (M.F.); NIH 1DP2 OD006477, 1R21 NS058600, and National Academies Keck Futures Initiative CS10 grants (S.C.H.); and NIH 1R01NS052830, 1R01NS064517, 1R01HL074267, Brain Tumor Society, Goldhirsh Foundation, and the Stanford Center for Children's Brain Tumors grants (C.J.K.). F.K., H.W., and C.J.K. have a patent pending regarding vascular applications of GPR124.

Supporting Online Material

www.sciencemag.org/cgi/content/full/330/6006/985/DC1
Materials and Methods
Figs. S1 to S20
References

16 August 2010; accepted 4 October 2010
10.1126/science.1196554